Cell Site Densification Using mmWave and sub-THz Line-of-Sight Wireless Fronthaul: A Deployment Feasibility Study

Dave Townend, Stuart D. Walker, Anvar Tukmanov and Andy Sutton

***Abstract*—This paper presents mobile network deployment analysis aimed at understanding the use of high frequency wireless fronthaul links to realize dense cell network architectures. A high resolution digital twin model is built based on real-world data sets to identify line-of-sight propagation paths between existing macro cell roof top sites and lamp post infrastructure locations suitable for new street level cell sites. The resulting line-of-sight path topology is used to simulate wireless fronthaul links based on industry standardized fronthaul interfaces across the urban environment. In considering the stringent fronthaul interface requirements for a representative 5G radio configuration, the suitability of emerging mmWave and sub-THz transport bands between 71.124 and 174.8 GHz to fulfill the wireless fronthaul centralized RAN deployment is analyzed. Findings in this work have demonstrated that with the right combination of fronthaul interface and spectrum band upto 73% of new street level cell sites in a dense deployment could be built using a wireless fronthaul transport solution.**

***Index Terms*—Cell-free, C-RAN, D-band, Line-of-Sight, Wireless Fronthaul.**

I. Introduction

THERE are many routes which mobile network operators may pursue in order to grow capacity and efficiency of the network [22][7]. This may come in the form of advanced antenna technology investments such as massive multiple-in multiple-out (mMIMO) where spectral efficiency may be improved without the need for additional spectrum resource [36]. Alternatively, capacity can be increased with the acquisition of new spectrum assets such as millimeter-wave (mmWave) to aid higher bandwidth services [40]. Finally, and perhaps the most forward looking of approaches is the deployment or re-deployment of the network itself. This may come in the form of physical deployment scenarios such as cell site densification or architectural re-design of the network topology to consolidate or coordinate functions [41].

Although the concepts of cell site densification and coordination are well established, it is the enabling technologies such as those specified in 5G standards which allow new architectures to become more economically realizable. The 'functional splits' initially outlined in 3GPP release 14 [2] define eight possible interface options in the radio access network (RAN) protocol stack between the traditional baseband unit (BBU) and radio unit. Such specifications address the diverse requirements in how mobile networks are architected and permit new flexibility on how the RAN components, now consisting of a centralized unit (CU), distributed unit (DU) and radio unit (RU), are deployed.

While there are many potential benefits to cell coordination including reduced interference, enhanced performance and energy saving, cells are inherently required to be tightly synchronized and connected via low latency interfaces to ensure signalling information remains accurate [14]. Such requirements in a conventional 'cell centric' deployment are typically unrealizable without significant redesign or investment [39]. As such, early cell coordination techniques such as coordinated multi-point (CoMP) introduced in 3GPP release 11 [1] have failed to gain traction in commercial networks to date. Despite this, the evolution of CoMP in 5G, referred to as multi transmission and reception points (M-TRPs) now greatly benefits from the new functional split specifications.

The extrapolation of RAN coordination finds a logical conclusion in the centralized RAN (C-RAN) architecture where coordinated or cooperative processing functions for multiple cells can be efficiently rationalized deeper in the network - a 'network centric' architecture. As such, the C-RAN architecture has gained significant interest in recent years with the aim of pooling baseband functions into geographically common locations [15]. In re-architecting the network towards a centralized topology not only do the advanced coordination techniques become easier to implement but they also present opportunities to further reduce operational costs by removing complexity away from distributed cell sites. As more baseband functionality is centralized, the requirements on the underlying transport network inherently increase as more of the RAN protocol stack is required to traverse the transport network between RU and DU. In this approach the conventional cell centric backhaul based transport network evolves into a network centric fronthaul driven solution.

The most novel research concepts looking beyond the established network centric models and toward a 'user centric' architecture are those topics commonly referred to as cell-free or cell-free mMIMO (CF-mMIMO) [8]. Cell-free architectures aim to address the scalability issues evident in network centric deployments. Although network centric approaches facilitate the coordination of geographically distributed cells, they are fundamentally limited by small fixed boundary regions or predefined cell clusters which share common baseband functions. In a cell-free model, the base station antennas may be distributed throughout the coverage area rather than constrained to large arrays at single sites. In doing so, users are served by dynamic and coherent joint-transmissions from multiple access points (APs) or TRPs within range. This concept effectively eliminates the cell boundaries resulting in no inter-cell

interference or inefficient inter-cell handover procedures. As with network centric approaches, user centric architectures are also fully dependent on high capacity, low latency fronthaul transport interfaces with the centralized central processing unit (CPU) locations, these approaches however, also come with many open practical and scalability challenges [37], [28].

The well recognized problem with all such centralized architectures is that the ideal ubiquitous fiber fronthaul connectivity is typically not realistic in real network deployments. Significant investment in urban street works would be necessary to support the mass street level deployment of small cells or remote RU sites needed to fulfill the anticipated site density requirements. The evolving concept of wireless fronthaul however, offers the potential for greater flexibility of cell site deployment where remote RUs are wirelessly connected to centralized baseband locations in lieu of fiber connectivity. The main challenges with wireless fronthaul is whether such transmission links can realistically support the high data rate, low latency, high availability requirements of fronthaul interfaces and whether such links (assumed to be dedicated point-to-point) can be reliability designed and deployed in dense urban environments. Industry momentum in the standardization of packet based fronthaul protocols at various split points such as eCPRI option 8 [16], O-RAN option 7.2x [38] and Small Cell Forum (SCF) option 6 [44] promise better utilization of generic transport solutions using established Ethernet transport protocols. Such standardization, together the harmonization of new high capacity millimeter-wave and sub-THz spectrum bands including E-band (71.125-85.875 GHz) [29], W-band (92-114.25 GHz) and D-band (130-174.8 GHz) [12] presents an opportunity to realize these challenging new architectures using complimentary wireless transport solutions as a more cost efficient and flexible fronthaul solution.

II. Related Work

The extent to which wireless fronthaul could be utilized in C-RAN deployments has previously been studied from a number of perspectives. The suitability of mmWave fronthaul to support user-centric cell groupings has been studied from a theoretical perspective in [18] where a data rate optimization approach is used to demonstrate performance comparable to optical fiber. The performance requirements for low layer split fronthaul interfaces delivered over wireless transport has also been studied in [34] and [13]. Here, enabling technologies such as fronthaul compression and line-of-sight MIMO are explored in order to fulfill the transport requirements using radio solutions. In [46], emerging candidate fronthaul interfaces and spectrum bands are studied to support a wireless fronthaul dimensioning exercise and demonstrate the potential link lengths achievable. In [35], a number of mmWave bands are also explored where it is concluded that the requirements of higher layer split fronthaul interfaces could be met with existing bands below 100 GHz whilst suggesting lower layer splits would need to be addressed with spectrum bands above 100 GHz due to the more demanding latency requirements. The data rate requirements of various fronthaul splits are also calculated for a range of 5G cell configurations in [43] where requirements are compared with simulation results of the available capacity from various channel bandwidths operating at 105 GHz and 220 GHz sub-THz bands. The results of this study also conclude that lower layer splits such as option 8 and 7.1 are challenging for wireless fronthaul due to the very short $<$100 m link lengths possible. The planning challenges of realizing high frequency line-of-sight (LoS) fronthaul links in urban environments has been briefly studied in [25] and [24] and statistically in [45] whilst a DU placement scheme is proposed in [26] as a means of incorporating lower cost and more flexible wireless fronthaul multi-hop links as an alternative to fiber optic transport. The most related work studied in [47] outlines the ideal deployment characteristics of a generic multi-hop wireless transport solution for a variety of cell densities in a dense urban network but without consideration to any specific technology selection.

While literature to date has identified many of the challenges with wireless fronthaul in C-RAN, there is a conspicuous absence of feasibility analysis which combines all such areas. This is especially true for deployment analysis in real-world urban environments where cell densification is considered most essential. To address these literature gaps and understand the feasibility of wireless fronthaul and the sensitivity to technology selection, a wider analysis is necessary such as that proposed in this work. The environmental model and line-of-sight topology findings from [47] and the fronthaul dimensioning analysis in [46] serve as a framework for the deployment feasibility study presented in this paper which considers all the transport requirements and capabilities in a real network setting for the first time.

III. Organisation

In this study we consider the use of existing macro cell base station sites as preferred edge aggregation sites for CU / DU baseband as outlined in Fig.1. This represents a more realistic early deployment scenario where small RU clusters or localized distributed MIMO sites could be coordinated as a first step towards the ideal centralized or cell-free network. In this scenario, as centralization grows the baseband / CPU capability can be redeployed deeper in the network and the traditional macro cell site simply becomes an aggregation point for a multitude of distributed RUs and its conventional backhaul link evolves into a fronthaul connection to the next tier of centralized processing.

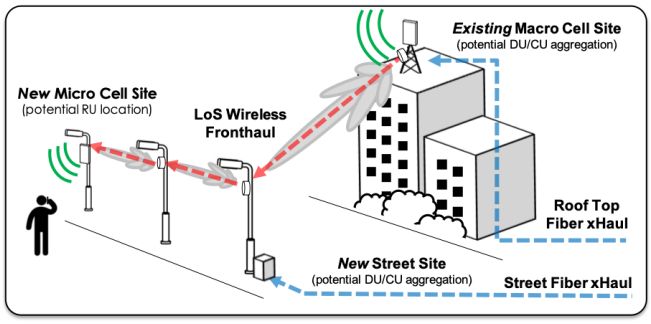

Fig. 1. Example deployment scenario with potential baseband and fiber aggregation points extended using multi-hop wireless fronthaul.

In Section IV a detailed 3D environmental model is presented and used to identify all of the unobstructed LoS propagation paths between potential infrastructure sites as a good approximation of viable mmWave or sub-THz point-to-point wireless fronthaul links. A cell site densification model is also presented which increases the cell density of the model to a 200 m inter-site distance (ISD) using new lamp post based cell sites. In Section V the transport performance requirements for range of standardized fronthaul interfaces are defined which serve as connectivity requirements for any new cell sites added to the model. The complementary wireless fronthaul transport capability of candidate spectrum bands are derived in Section VI where the anticipated data rate, latency, jitter and link lengths possible are used as cost / routing metrics when connecting new cell sites via the LoS paths in the model. The deployment feasibility results from the model are discussed in Section VII where the optimum combination of fronthaul interface and wireless spectrum band are identified which maximize the use of wireless fronthaul whilst also maximizing the centralization potential using the lowest possible fronthaul interface.

IV. Wireless Fronthaul Deployment Model

The feasibility of wireless fronthaul multi-hop transport in a dense RAN deployment is assessed using a representative 2.5 sq km study area of central London. Firstly, an environmental model (digital twin) is built based on high resolution (0.5 m) 3D LiDAR (light detecting and ranging) survey data publicly available from the UK Department for Environmental and Rural Affairs [19]. This approach provides sufficient resolution to capture detailed urban features such as foliage and street canyon obstructions as shown in Fig.2 which are typically missing in similar studies but are crucial for accurate LoS blockage and propagation analysis. Limitations with this approach do however mean that environmental detail below the canopy that allow propagation paths under trees or bridges could be missed.

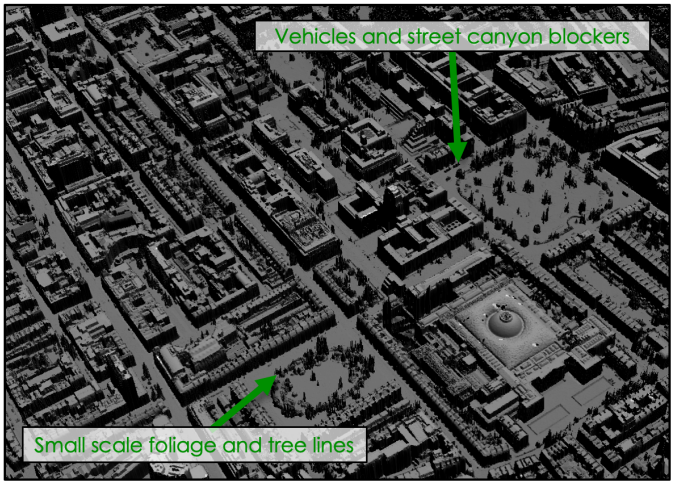

Fig. 2. Digital surface model 3D rendering of central London.

The model is complimented with the accurate location and height data of 35 existing real roof top macro cell sites in the area and 2226 street level lamp posts. Potential wireless fronthaul links are simulated using a direct propagation path methodology where vector lines are constructed between each rooftop macro cell and the surrounding lamp posts (within their Voronoi cell boundaries) in addition to paths between neighboring lamp posts (within a 200 m radius of each other). Any paths unobstructed by the underlying environmental model are classified as LoS and deemed suitable for use as a potential high frequency wireless fronthaul link. In total 136,578 validated propagation paths make up a wireless LoS fronthaul topology map of the area. The resulting system model as highlighted in Fig.3 shows the full mesh topology of potential LoS paths across the urban landscape where the optimum link routes can be identified to help quantify the deployment feasibility of new wireless fronthaul based cell sites installed on lamp post infrastructure.

A. Cell Densification Model

The wireless fronthaul feasibility in this study is based on a high density deployment of new street cells. New lamp post based cells (RUs) are sequentially added to the topology map using the approach outlined in [47] with the aim of maximizing the reduction in the mean inter-site distance (ISD) of the area. In addition to the Voronoi boundaries which represent the logical cell edge of each cell site, a Delaunay triangulation is constructed between all cell locations in the model. The Delaunay triangulation edges represent the ISD between neighbor cells. The starting point is the baseline inter-site distance (ISD) provided by the existing 35 rooftop macro cell sites with a mean ISD of 305 m as shown in Fig. 4. The cell densification model is designed to identify the 'optimum site location' at the incentre of the largest Delaunay triangle and sequentially add a new street level small cell to the 'closest lamp post site' thus maximizing the reduction in the overall ISD. The cell densification optimization algorithm aims to maximize the reduction in the current ISD distribution iterating one new cell at a time until the target ISD is met - here we set a target 200 m ISD which is aligned with 3GPP recommendations for urban micro cell ISD density [3]. For each new site identified the ability to connect (fronthaul) it across the LoS topology graph towards an a existing fiber site (further described in Section VII) can be studied. To meet the target ISD of 200 m, 45 new street level sites are added to the study area as shown in Fig. 5.

Once all new cells are added, the 3D environmental model can be simplified into a 2D graph where vertices represent potential infrastructure locations and the edges represent the valid LoS paths between them which could potentially support a high frequency wireless fronthaul solution. Each new lamp post based cell site added to the graph represent (source) nodes which require fronthaul connectivity to a fiber aggregation point (the performance requirements of which are discussed in Section V). The existing macro sites in the graph represent (target) nodes already with fiber connectivity. All other nodes in the graph are remaining lamp posts which may be passed through or traversed as 'relay' or 'multi-hop' nodes via the graph edges. The graph edges nominally represent physical

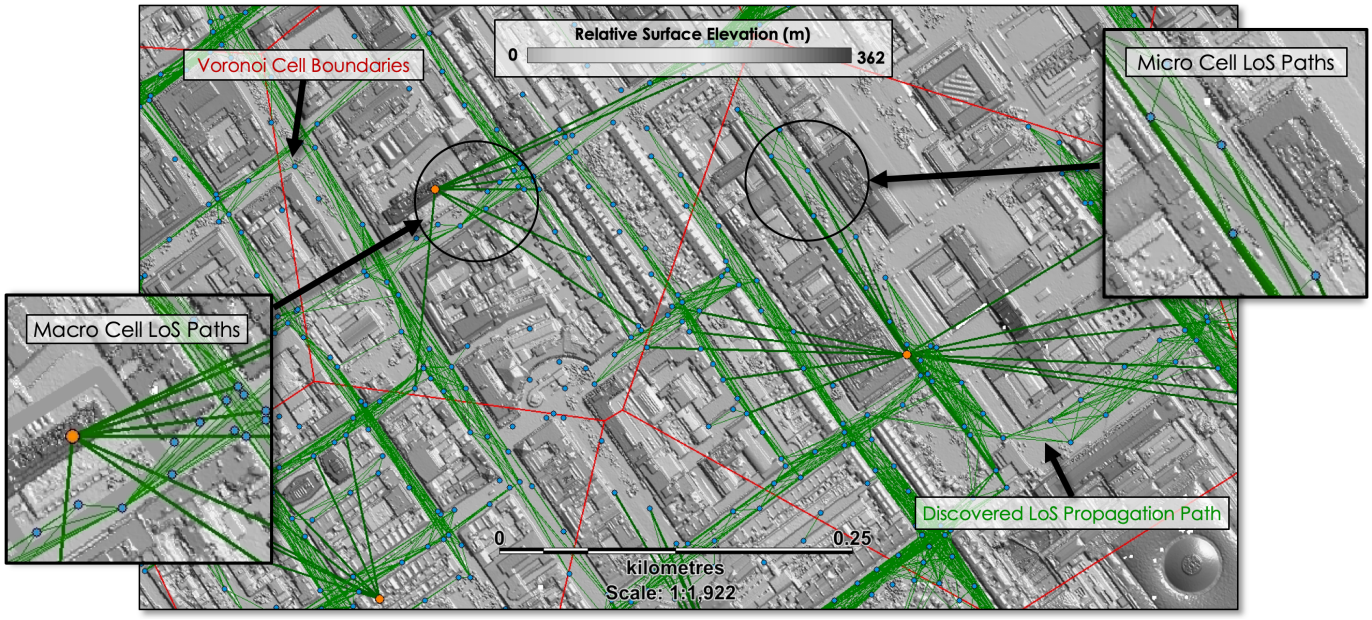

Fig. 3. Digital surface model 2D representation of central London with LoS path discovery.

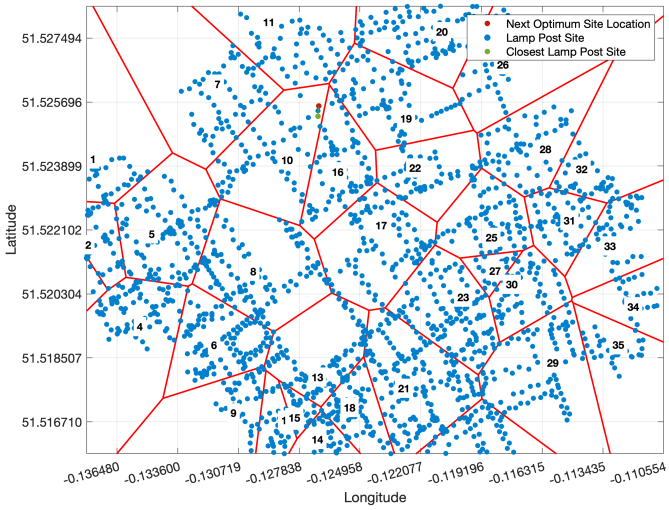

Fig. 4. Cell boundaries of study area at 305 m ISD (35 existing macro cells).

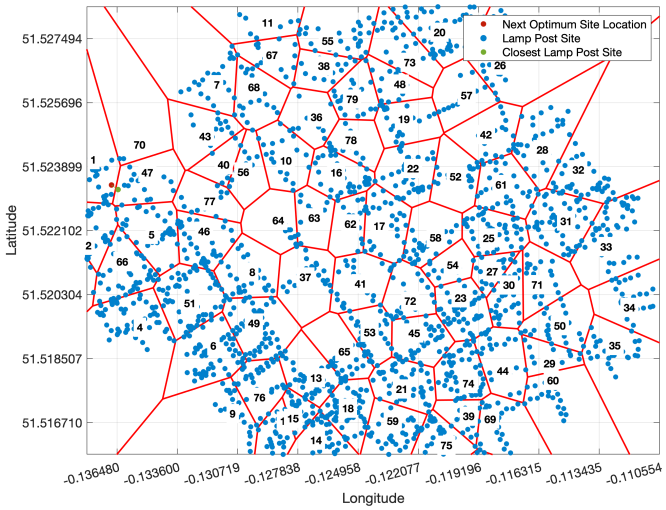

Fig. 5. Cell boundaries built to 200 m ISD (45 new small cell sites added).

distances in the 3D environmental model but for subsequent feasibility analysis, equate to a path cost / weighting tied to the performance capabilities of candidate wireless transport solutions (E, W and D-band) - described in Section VI. Although the model does not directly account for secondary propagation effects such as potential interference between link hops as conventional planning tools might, these effects are mitigated due to the spectrum bands of interest where it is assumed that high frequency reuse and sufficient spectrum availability facilitate simple channel plans between adjacent hops. In addition, the short link distances and high frequencies mean worse case Fresnel zones are below the resolution of the environmental model and can thus be negated for any validated LoS paths.

V. Wireless Fronthaul Transport Requirements

The transport requirements for each new cell added to the graph are based on a number of performance metrics tied to the fronthaul interfaces under consideration - specifically data rate, latency and jitter. The cell configuration and fronthaul interface choice therefore dictate the multi-parameter routing metric for which a LoS wireless transport solution must meet (in one hop or more) if the cell is to be deployed using wireless fronthaul. In this study we assume a basic 8 antenna, 100 MHz channel bandwidth 5G RU is deployed at each new street level lamp post cell site with a configuration as shown in Table. I. We consider three different transport requirements based on the three major standardized or semi-standardized fronthaul interfaces; eCPRI split E (3GPP option 8), O-RAN 7.2x (3GPP option 7.2) and SCF nFAPI (network functional application

platform interface) (3GPP option 6).

A. Fronthaul Data Rate Requirement

The lowest 3GPP option 8 functional split interface minimizes the complexity of the RU but represents the most demanding transport requirements. The full radio interface I/Q is sampled and quantized to produce a constant bit rate interface which scales with antennas and channel bandwidth (FFT size). This interface is realizable with carrier grade Ethernet transport using eCPRI split E [16] specifications. The data rate requirement D_{eCPRI_E} is defined in (1) where N_{ant} is the number of antenna ports on the RU, fs is the sampling frequency and M which is the number of quantizer bits per I and Q (conventionally 15 bit). Additional overheads are included from control and management words per CPRI frame (1/16) CM_{CPRI} and Ethernet framing OH_{ETH} and eCPRI header encapsulation OH_{eCPRI}.

$$D_{eCPRI_E} = N_{ant} \cdot\ fs \cdot\ 2M \cdot\ CM_{CPRI} \cdot\ OH_{ETH} \cdot\ OH_{eCPRI} \tag{1}$$

The O-RAN 7.2x interface reduces the required interface bandwidth relative to option 8 through resource element mapping functions remaining in the RU. Although this requires more processing in the RU, it means only user occupied resource elements have to pass over the fronthaul connection resulting in a variable bit rate interface. The transport data rate $D_{ORAN7.2x}$ can be calculated from (2) where the data rate becomes a function of the MIMO layers N_{layers} and resource block allocation N_{PRB} in operation. In O-RAN, I/Q block floating point compression is used where each sub-carrier $N_{SCperRB}$ I and Q sample are compressed to a signed bitwidth $M_{mantissia}$ and unsigned exponent $M_{exponent}$. The necessary transport protocols for this split also introduce Ethernet framing OH_{ETH} and eCPRI encapsulation OH_{eCPRI} overhead. In addition, control plane overheads OH_{CP} are necessary to carry the resource block assignment and beamforming information between DU and RU [38].

$$D_{ORAN7.2x} = (N_{layers} \cdot\ N_{PRB}) \cdot\ (N_{SCperRB} \cdot\ 2M_{mantissa} + M_{exponent}) \cdot\ T_{SymPerSlot}^{-1} \cdot\ OH_{CP} \cdot\ OH_{ETH} \cdot\ OH_{eCPRI} \tag{2}$$

The PHY/MAC split option 6 is offered by the Small Cell Forum under the nFAPI specification. This further reduces the transport data rate requirement $D_{nFAPI_{NR}}$ by only carrying the MAC transport blocks to the RU. The data rate requirement in (3) is thus dependent on the number of MIMO layers N_{layers} and Transport Block Size TBS in use which in turn is dictated by the modulation and coding scheme index I_{MCS} and scheduled Resource Blocks N_{PRB} being utilized on the radio interface. For 5G NR the TBS calculation is made using formulas as defined in 3GPP TS 38.214 [6]. The nFAPI specification also defines a message API between MAC and PHY layers and so requires an nFAPI encapsulated control plane overhead OH_{CP} with an associated L4 transport header OH_{nFAPI} in addition to the necessary L3 IP overhead OH_{IP} and L2 Ethernet framing overheads OH_{ETH}.

$$D_{nFAPI_{NR}} = N_{layers} \cdot\ (TBS \cdot\ T_{slot}^{-1}) \cdot\ OH_{CP} \cdot\ OH_{ETH} \cdot\ OH_{IP} \cdot\ OH_{nFAPI} \tag{3}$$

B. Fronthaul Latency and Jitter Requirement

5G fronthaul transport specifications such as 802.1CM [27], O-RAN and eCPRI define a range of latency classes depending on how the RU is configured. The permissible fronthaul delay budget can vary between 25 μs for low latency communication use cases to 500 μs for larger latency deployments requiring longer transport propagation delays or switching delay in multi-hop transport networks. For a typical 'Full NR Performance' cell as assumed in this study, these specifications are aligned with a one-way delay requirement of 100 μs. Any control plane traffic required for scheduling and beamforming generally have a much greater latency tolerance ranging from between 1 ms and 100 ms.

For packet based fronthaul the maximum delay variation (jitter) requirements are typically dependent on the timing error budget of the RAN. Existing timing and synchronization protocols such as PTP G.8275.1 [33] are utilized to meet the necessary 3GPP time alignment error (TAE) specifications [4], [5]. As a result, the TAE and timing accuracy requirements between DU and RU or cooperative RUs is defined by the RAN feature set or configuration of the radio interface. The time error budget to meet the 3GPP TAE targets are also derived in 802.1CM where for the 100 MHz 5G RU assumed in this study (supporting intra-band contiguous carrier aggregation) the maximum delay variation is 190 ns [32], [38], [17].

TABLE I
EXAMPLE CELL CONFIGURATION AND ASSOCIATED FRONTHAUL PERFORMANCE REQUIREMENTS.

	5G NR (FR1)
Channel Bandwidth (MHz)	100
SC Spacing (kHz)	60
SC Per RB [$N_{SCperRB}$]	12
RB Bandwidth (kHz)	720
Resource Blocks [N_{PRB}]	135
Subcarriers [N_{SC}]	1620
Symbols per Slot [$N_{SymPerSlot}$]	14
Slot Length [T_{slot}] (ms)	0.00025
Sym Period per Slot [$T_{SymPerSlot}$] (μs)	17.9
FFT Size	2048
Sampling Frequency [fs] (MHz)	122.88
I/Q Quantizer Bits [M]	15
Mantissa Bits [$N_{mantissa}$]	9
Exponent Bits [$N_{exponent}$]	4
Antennas [N_{ant}] (UL/DL)	2/8
MIMO Layers [N_{layers}] (UL/DL)	2/4
Modulation Index [I_{MSC}] (UL/DL)	28/27
Data Rate Requirement Option 8 ($Gbps$)	**30.58**
Data Rate Requirement Option 7.2x ($Gbps$)	**7.59**
Data Rate Requirement Option 6 ($Gbps$)	**2.59**
Latency Requirement (μs)	**100**
Jitter Requirement (ns)	**190**

VI. WIRELESS FRONTHAUL TRANSPORT CAPABILITY

The routing metric necessary for traversing each hop in the LoS deployment topology graph is built based on the link budget for each wireless fronthaul transport band considered (E,

W and D-band) and the associated performance characteristics of experimental measurement extrapolations from [46]. The system configuration assumptions for the wireless transport options are detailed in Table II where we assume FDD operation utilizing vertical polarization and a channel raster aligned with ITU specifications. For E-band, the maximum channel size currently specified by the ITU is 2 GHz with a duplex spacing of 10 GHz. For W-band and D-band, as channel arrangements in these bands are not fully harmonized, radio configurations are aligned with industry expectations in [21] where a 2 GHz channel size is used for W-band with a duplex spacing of 11.55 GHz [11] and 5 GHz for D-band with a duplex spacing of 15.50 GHz [10].

A. Wireless Fronthaul Link Budget

The required system gain as a function of link distance for each band is given in Fig. 6 which is based on the assumptions as outlined in Table II. The generalized path loss PL for carrier frequency f_{MHz} at link distance d_{km} is given in (4) where the availability target for a wireless fronthaul based transport solution is assumed to be 99.99%. To meet this availability target the atmospheric adsorption fade margin contributions are modeled using ITU-R recommendations in [30]. Here, water vapor attenuation γ_w and gaseous adsorption γ_o contributions in dB/km are calculated based on an atmospheric pressure of 101.3 kPa, temperature of 15°C and a water vapor density of 7.5g/m^3. The fade margin requirement to account for precipitation loss γ_R in dB/km is again modelled using ITU-R recommendations in [31] where rain rates are aligned with ITU rain zone F for peak rainfall of 25 mm/hr.

$$PL = 32.4 + (20 \cdot (\log f_{MHz})) + (20 \cdot (\log d_{km})) + (d_{km} \cdot (\gamma_w + \gamma_o + \gamma_R)) \quad (4)$$

The receive sensitivity of each system is aligned with ETSI fixed radio system technical report parameterization in [20] where a minimum of QPSK and maximum of 256 QAM modulation is used. The resulting minimum received signal level for each modulation step RSL_{mod} is based on channel bandwidth size BW_{MHz} and modulation rate signal-to-noise ratio SNR_{mod} given in (5). While ETSI examples provide recommendations for typical noise figure NF and industrial margin IM_F up to E-band frequencies, W and D-band figures have been taken from literature where prototypes measurements suggest a noise figure in the order of 10 dB [9] or lower [48] are possible using SiGe semiconductor technology. As these figures do not likely represent a commercialized solution at cost, a more conservative noise figure of 13 dB is assumed. Whilst the transmit output power and antenna gain for E-band represent typical values for commercial solutions, expectation for equivalent future W and D band parameters are again based on early prototype studies reported in literature [42] [23].

$$RSL_{mod} = -174 + 10 \cdot (\log_{10} BW_{MHz}) + NF + IM_F + SNR_{mod}$$

Where

$$SNR_{mod} = 10 \cdot \left(\log_{10}\left(2^{BitsPerSymbol}\right) - 1\right) \quad (5)$$

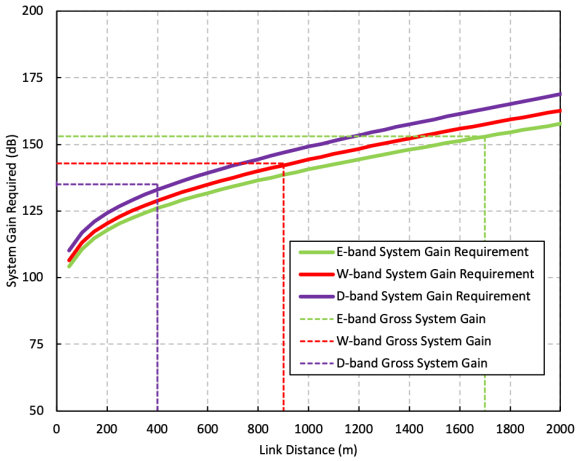

Fig. 6. System gain requirements for single hop wireless transport. Replicated from [46]

B. Wireless Fronthaul Data Rate Capability

The theoretical capacity that can be supported by the link budget for each modulation rate (in bits per symbol BPS) and for higher channel bandwidths BW_{GHz} representative of future W or D-band systems is calculated from (6) where the data stream coding schemes and coding rate overhead inefficiencies RS_{OH} and TC_{OH} are aligned with ETSI fixed radio system examples [20] and typical Ethernet framing ETH_{OH} inefficiencies are also considered. When applied to the link budget for each band the resulting theoretical capacity capability as a function of link distance is calculated as shown Fig. 7. The fronthaul data rate requirements for each fronthaul interface under consideration are also overlaid as defined in Section V.

$$TN\_Capacity_{Gbps} = (BPS \cdot BW_{GHz}) \cdot RS_{OH} \cdot TC_{OH} \cdot ETH_{OH} \quad (6)$$

C. Wireless Fronthaul Latency and Jitter Capability

The one-way delay (latency) and delay variation (jitter) of wireless transport solutions are more difficult to theoretically derive due the major factors influencing such performance being implementation specific. As such the latency and jitter performance expectations for Ethernet traffic traversing the full link budget of each wireless transport band are based on extrapolations of experimental measurements carried out in [46]. The model definitions in (7) and (8) are built on controlled and simulated fronthaul test traffic over a commercially available E-band link and extrapolated to account for the larger channel bandwidths possible in transport bands above E-band (namely W and D-band). The associated latency and jitter performance characteristics when applied to the link budgets of each band are shown in Fig. 8 and Fig. 9 respectively. Again, the fronthaul interface performance requirements are overlaid highlighting the maximum routing cost metric for each new cell placed into the deployment model.

TABLE II
SUMMARY OF WIRELESS TRANSPORT SYSTEM PARAMETERS.

	E-band		W-band		D-band	
	A-End	**B-End**	**A-End**	**B-End**	**A-End**	**B-End**
Frequency (MHz) [f_{MHz}]	72125	82125	95325	103125	143625	158625
Channel Bandwidth (MHz) [BW_{MHz}]	2000	2000	2000	2000	5000	5000
Water Vapour Attenuation (dB/km) [γ_w]	0.25	0.32	0.43	0.54	1.09	1.59
Gaseous Adsorption (dB/km) [γ_o]	0.20	0.06	0.03	0.04	0.02	0.02
Polarization	V	V	V	V	V	V
Rain Rate 99.99% Availability (mm/hr)	25	25	25	25	25	25
Rain Attenuation (dB/km) [γ_R]	10.62	11.30	11.90	12.07	12.51	12.74
Tx Radiated Power (dBm)	10.00	10.00	10.00	10.00	6.02	6.02
Tx Antenna / BF Gain (dBi)	40	40	35	35	35	35
Rx Antenna / BF Gain (dBi)	40	40	35	35	35	35
Rx Chain Losses (dB)	1.00	1.00	1.00	1.00	1.00	1.00
Rx Noise Figure (dB) [NF]	13.00	13.00	13.00	13.00	13.00	13.00
Industrial Margin (dB) [IM_F]	4.00	4.00	4.00	4.00	4.00	4.00
Min Rx Sensitivity (dBm)	**-63.99**	**-63.99**	**-63.99**	**-63.99**	**-60.01**	**-60.01**
Max System Gain (dB)	**152.99**	**152.99**	**142.99**	**142.99**	**135.03**	**135.03**

$$TN\_Latency_{\mu s} = (138 \cdot BW_{GHz}^{-0.8}) \cdot BPS^{(0.23 \cdot ln(BW_{GHz}))-0.52}, \quad 0.5 \leq BW_{GHz} \leq 5 \tag{7}$$

$$TN\_Jitter_{ns} = (1424 \cdot BW_{GHz}^{-0.7}) \cdot BPS^{(-0.43 \cdot BW_{GHz})-0.82}, \quad 0.5 \leq BW_{GHz} \leq 5 \tag{8}$$

For each of the candidate wireless transport bands (E, W and D-band) the fronthaul requirements are used to highlight the fronthaul link lengths for which the cell configuration assumed could be deployed with - Fig. 7, 8 and 9. These transport performance budgets serve as the upper limit for wireless fronthaul dimensioning and are subsequently combined into the routing metrics when adding new cell sites to the deployment model where the total transport performance budget may be consumed in one or more hops between potential infrastructure sites in the LoS topology graph.

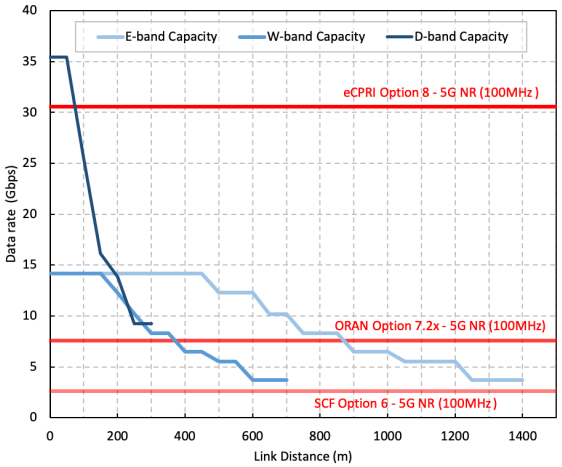

Fig. 7. Transport link data rate capability as function of distance (single hop).

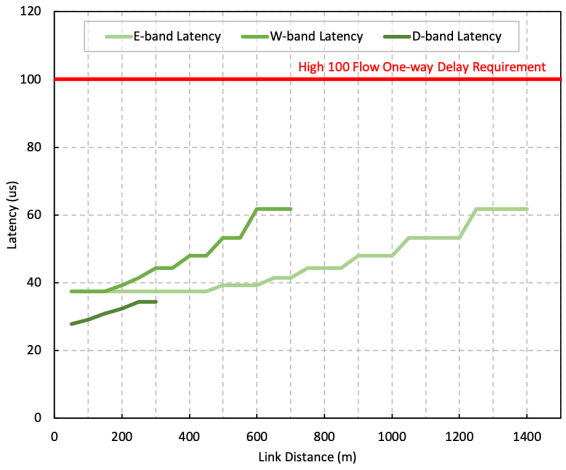

Fig. 8. Transport link latency capability as function of distance (single hop).

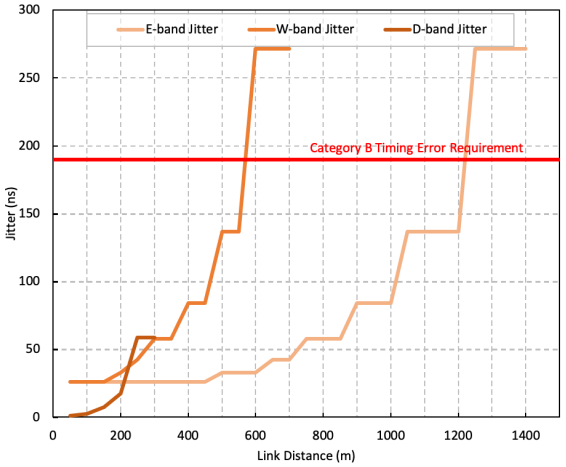

Fig. 9. Transport link jitter capability as function of distance (single hop).

VII. DEPLOYMENT MODEL SCENARIO

Using the transport requirements and capabilities derived in Sections V and VI the optimal combination of fronthaul

interface and wireless transport solution can be identified based on the ability to satisfy connectivity between each new cell site and existing fiber node locations. The primary deployment scenario considered is where all existing macro cell roof top sites are assumed to have suitable baseband or fiber aggregation capability to terminate newly deployed cells. New cells can connect to these aggregation points by traversing the LoS graph topology using the wireless transport link budget and associated performance metrics. A shortest path algorithm is utilized to identify the fewest hops required to join new sites to potential fiber nodes in the graph. If the new cell is unable to reach a fiber node because the fronthaul performance budget cannot be met then the new cell site also becomes a fiber / baseband aggregation node and also becomes available for subsequent cells to connect to. This scenario represents a cost orientated approach where it is assumed wireless transport is preferential to fiber as it negates the high cost and time expenditure of road closures and civil works associated with laying new fiber in busy urban locations.

A. Wireless Fronthaul Deployment Feasibly Results

In the deployment scenario considered, the model is allowed to route fronthaul connectivity from each newly added site to any available fiber location that already exists in the topology via the LoS paths. These results are summarized for each candidate band in terms of the deployment topologies in Fig. 10, 12 and 14 (where the site node coloring is given for the best case wireless deployment) and in Fig. 11, 13 and 15 for hop count proportion for each fronthaul option. Results are also tabulated with further detail in Table III highlighting performance reasons why wireless transport could not be utilized on sites where fiber was necessary.

Results highlight that the use of the option 8 fronthaul interface (eCPRI split E) would severely limit the potential to utilize wireless fronthaul between new sites and existing fiber sites. Only 11% of new sites (4 out of 45) were able to support an option 8 fronthaul link using a D-band solution. No sites at all were able to supported option 8 using either W or E-band transport. The detailed analysis in Table III further highlights that all option 8 links unable to utilize a wireless solution failed due to capacity constraints reasons. This emphasizes that the option 8 interface represents an unrealistic technology selection for the wireless transport implementations envisaged.

The use of O-RAN option 7.2x and SCF option 6 however, is more promising. Analysis has shown that as much as 73% of new sites (33 out of 45) could be connected by utilizing a D-band solution and 49% (22 out of 45) if using either W or E-band. Notably, the results for option 7.2 and 6 for W and E-band combinations are identical. These results demonstrate that it is the link bandwidth which is fundamentally dictating support for these fronthaul interfaces. The link budget and atmospheric availability differences between these bands is not a significant factor in the ability to support these fronthaul links - a maximum link length of 237 m is observed. As these bands are configured with an equivalent channel bandwidth the deployment opportunity remains identical. While this may suggest these bands could be used interchangeably, in reality the larger amount of spectrum available in W-band means that more 2 GHz channels are possible relative to E-band which is particularly relevant when considering support for multiple co-located licensees (mobile network operators). In addition, whilst the relative differences in interface choice between O-RAN option 7.2x and SCF option 6 is not obvious from the deployment analysis, the reduced radio functionality of SCF option 6 (where higher order MIMO and advanced transmission schemes are not envisaged in the 5G nFAPI specifications) perhaps limit its long term potential in more advanced coordinated cell schemes.

The choice of spectrum band for wireless fronthaul is clearly weighted towards D-band operating between 130 GHz and 174.8 GHz.Analysis suggests that the greater potential of D-band when utilizing option 7.2x and 6 can be attributed to higher performing individual links which provide sufficient performance margin to support additional hops relative to W and E-band. Results show that D-band is able to support 3 hop fronthaul chains in this scenario whereas W and E band are unable to utilize more than 2 hops before the associated performance budget is exhausted. As a result the combination of D-band and option 7.2x represents the optimal solution for maximizing the possibility of wireless transport whilst also maximizing the opportunity for centralization through use of the lowest possible fronthaul interface.

VIII. Conclusions

In this paper we contribute new insights into the deployment feasibility of C-RAN based cell site densification supported by a wireless fronthaul transport capability. The most ideal transport technology selection is assumed to be a fronthaul interface which utilizes the lowest functional split possible to maximize multi-cell coordination together with a spectrum band which maximizes a wireless fronthaul footprint in order to reduce expenditure on new urban fiber installations. Based on these high-level assumptions, findings have demonstrated that the most appropriate deployment scenario would be exploitation of D-band spectrum (130-174.8 GHz) and use of an option 7.2x cell fronthaul interface to aggregate remote RUs to fiber locations. Results have shown that in spite of the demanding transport requirements imposed by new fronthaul interfaces, the anticipated performance of emerging wireless transport solutions operating in high mmWave and sub-THz spectrum bands, in particular D-band, are a credible option to supporting realistic wireless fronthaul deployments in C-RAN architectures.

References

[1] 3GPP. *TR 36.819 V11.2.0 Coordinated multi-point operation for LTE physical layer aspects*. 2013.

[2] 3GPP. *TR 38.801 V14.0.0 Study on new radio access technology: Radio access architecture and interfaces*. 2017.

[3] 3GPP. *TR 38.900 V14.3.0 Study on channel model for frequency spectrum above 6GHz*. 2017.

[4] 3GPP. *TS 36.104 V17.7.0 Evolved Universal Terrestrial Radio Access (E-UTRA); Base Station (BS) radio transmission and reception*. 2022.

[5] 3GPP. *TS 38.104 V17.7.0 NR; Base Station (BS) radio transmission and reception*. 2022.

[6] 3GPP. *TS 38.214 V17.3.0 NR; Physical layer procedures for data*. 2022.

TABLE III
SUMMARY OF PERFORMANCE LED DEPLOYMENT MODELLING.

Scenario		Option 8				Option 7.2x				Option 6			
		Wireless Sites		Fibre Sites		Wireless Sites		Fibre Sites		Wireless Sites		Fibre Sites	
		Total	Hops	Total	Reason	Total	Hops	Total	Reason	Total	Hops	Total	Reason
Roof and Street Level Wireless Fronthaul Extension	**D-band**	11.1%	0%(1) 20%(2) 80%(3)	88.9%	100%(C)	73.3%	18%(1) 49%(2) 33%(3)	26.7%	17%(C) 83%(L)	73.3%	18%(1) 49%(2) 33%(3)	26.7%	17%(C) 83%(L)
	W-band	0.0%	-	100.0%	100%(C)	48.9%	27%(1) 73%(2)	51.1%	9%(C) 91%(L)	48.9%	27%(1) 73%(2)	51.1%	9%(C) 91%(L)
	E-band	0.0%	-	100.0%	100%(C)	48.9%	27%(1) 73%(2)	51.1%	9%(C) 91%(L)	48.9%	27%(1) 73%(2)	51.1%	9%(C) 91%(L)

Reason for fiber connectivity: (C) Capacity constrained (if wireless), (L) Latency constrained (if wireless), (J) Jitter constrained (if wireless)
■ Deployment scenario representing maximum wireless transport utilization and maximum opportunity for RAN centralisation (lowest fronthaul split).

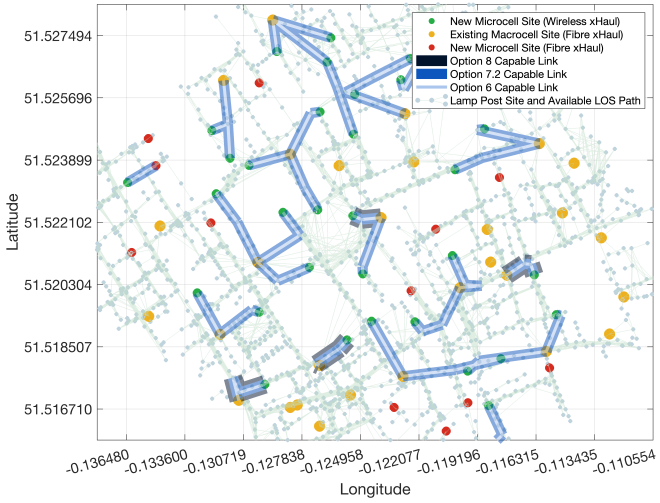

Fig. 10. Deployment topology using D-band transport.

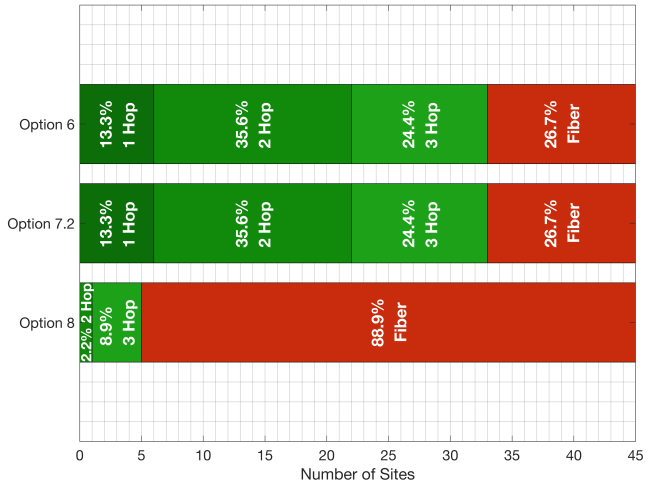

Fig. 11. Deployment statistics using D-band transport.

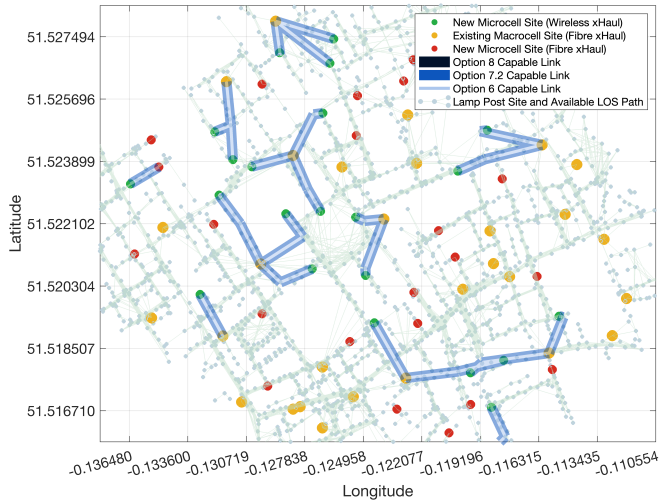

Fig. 12. Deployment topology using W-band transport.

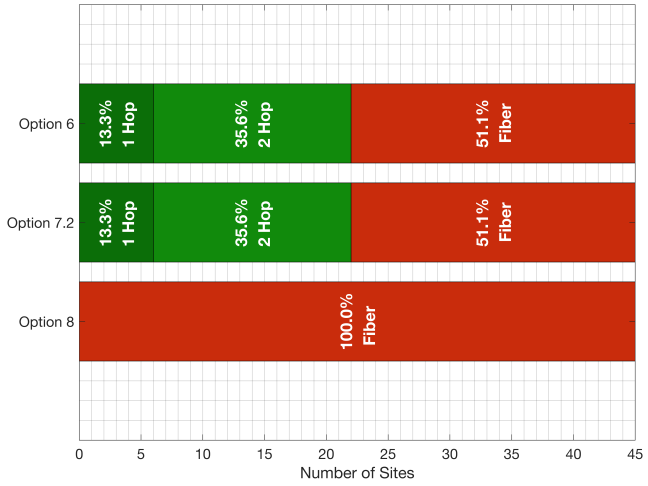

Fig. 13. Deployment statistics using W-band transport.

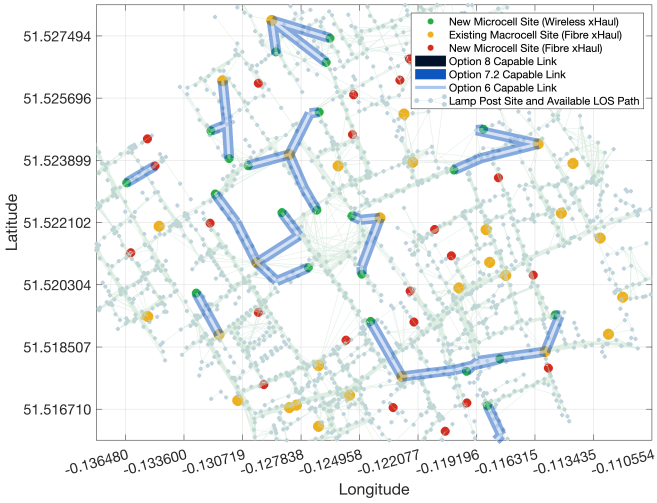

Fig. 14. Deployment topology using E-band transport.

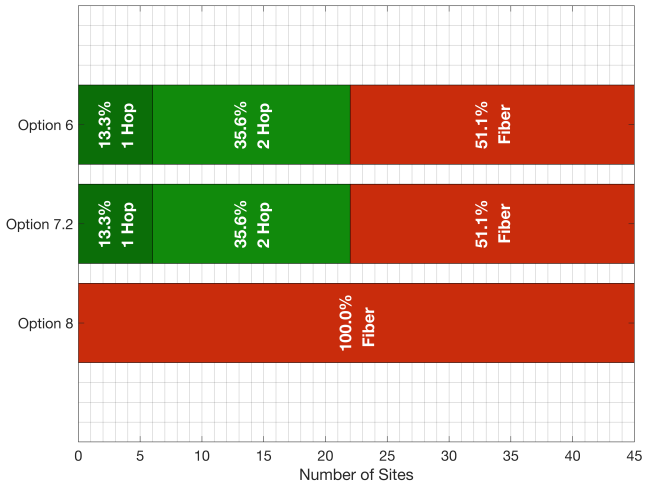

Fig. 15. Deployment statistics using E-band transport.

[7] Mamta Agiwal, Abhishek Roy, and Navrati Saxena. "Next Generation 5G Wireless Networks: A Comprehensive Survey". In: *IEEE Communications Surveys and Tutorials* 18.3 (2016), pp. 1617–1655. DOI: 10.1109/COMST.2016.2532458.

[8] Hussein A. Ammar et al. "User-Centric Cell-Free Massive MIMO Networks: A Survey of Opportunities, Challenges and Solutions". In: *IEEE Communications Surveys and Tutorials* 24.1 (2022), pp. 611–652. DOI: 10.1109/COMST.2021.3135119.

[9] M. Babay et al. "Sub-THz Radio Communication Links From Research to Field Trial". In: *2022 52nd European Microwave Conference (EuMC)*. 2022, pp. 780–783. DOI: 10.23919/EuMC54642.2022.9924270.

[10] CEPT. *ECC Recommendation (18)01 - Radio frequency channel/block arrangements for Fixed Service systems operating in the bands 130-134 GHz, 141-148.5 GHz, 151.5-164 GHz and 167-174.8 GHz*. 2018.

[11] CEPT. *ECC Recommendation (18)02 - Radio frequency channel/block arrangements for Fixed Service systems operating in the bands 92-94 GHz, 94.1-100 GHz, 102-109.5 GHz and 111.8-114.25 GHz*. 2018.

[12] CEPT. *ECC Report 282 - Point-to-Point Radio Links in the Frequency Ranges 92- 114.25 GHz and 130-174.8 GHz*. 2018.

[13] Juergen Cezanne et al. "Design of Wireless Fronthaul With mmWave LOS-MIMO and Sample-Level Coding for O-RAN and Beyond 5G Systems". In: *IEEE Open Journal of the Communications Society* (2023), pp. 1–1. DOI: 10.1109/OJCOMS.2023.3308713.

[14] Aleksandra Checko et al. "Cloud RAN for Mobile Networks—A Technology Overview". In: *IEEE Communications Surveys and Tutorials* 17.1 (2015), pp. 405–426. DOI: 10.1109/COMST.2014.2355255.

[15] Aleksandra Checko et al. "Cloud RAN for Mobile Networks—A Technology Overview". In: *IEEE Communications Surveys and Tutorials* 17.1 (2015), pp. 405–426. DOI: 10.1109/COMST.2014.2355255.

[16] CPRI Cooperation. *eCPRI Specification V2.0*. 2019. URL: http://www.cpri.info/spec.html.

[17] CPRI Cooperation. *eCPRI Transpot Requirements V1.2*. 2018. URL: http://www.cpri.info/spec.html.

[18] Umut Demirhan and Ahmed Alkhateeb. "Enabling Cell-Free Massive MIMO Systems With Wireless Millimeter Wave Fronthaul". In: *IEEE Transactions on Wireless Communications* 21.11 (2022), pp. 9482–9496. DOI: 10.1109/TWC.2022.3177186.

[19] Department for Environment, Food and Rural Affairs. *Defra Data Services Platform Surveys*. 2019. URL: https://environment.data.gov.uk.

[20] ETSI. *TR 101 854 v2.1.1 Fixed Radio Systems; Point-to-point equipment; Derivation of receiver interference parameters useful for planning fixed service point-to-point systems operating different equipment classes and/or capacities*. 2019.

[21] ETSI, mWT ISG. *Analysis of Spectrum, License Schemes and Network Scenarios in the D-band*. 2018. URL: https://www.etsi.org/committee/1426-mwt.

[22] Naser Al-Falahy and Omar Y. Alani. "Technologies for 5G Networks: Challenges and Opportunities". In: *IT Professional* 19.1 (2017), pp. 12–20. DOI: 10.1109/MITP.2017.9.

[23] Mario G. L. Frecassetti et al. "D-Band Backhaul and Fronthaul Solutions for 5G Radio Access Network". In: *2022 52nd European Microwave Conference (EuMC)*. 2022, pp. 772–775. DOI: 10.23919/EuMC54642.2022.9924325.

[24] Shoichiro Furukawa, Ryo Okumura, and Akihiko Hirata. "Evaluation of Availability of 300-GHz-Band Wireless Fronthaul Link during Torrential Rain". In: *2022 IEEE International Workshop on Electromagnetics: Applications and Student Innovation Competition (iWEM)*. 2022, pp. 112–113. DOI: 10.1109/iWEM52897.2022.9993587.

[25] Akihiko Hirata. "Automatic Deployment Planning of 300-GHz-Band Wireless Fronthaul Link in Metropolitan Areas". In: *2021 International Symposium on Antennas and Propagation (ISAP)*. 2021, pp. 1–2. DOI: 10.23919/ISAP47258.2021.9614556.

[26] Daisuke Hisano et al. "Deployment Design of Functional Split Base Station in Fixed and Wireless Multihop Fronthaul". In: *2018 IEEE Global Communications Conference (GLOBECOM)*. 2018, pp. 1–6. DOI: 10.1109/GLOCOM.2018.8647413.

[27] "IEEE Standard for Local and metropolitan area networks – Time-Sensitive Networking for Fronthaul". In: *IEEE Std 802.1CM-2018* (2018), pp. 1–62. DOI: 10.1109/IEEESTD.2018.8376066.

[28] Giovanni Interdonato, Pal Frenger, and Erik G. Larsson. "Scalability Aspects of Cell-Free Massive MIMO". In: *ICC 2019 - 2019 IEEE International Conference on Communications (ICC)*. 2019, pp. 1–6. DOI: 10.1109/ICC.2019.8761828.

[29] ITU-R. *F.2006 Radio-frequency channel arrangements for fixed wireless systems operating in the 71-76 and 81-86 GHz bands*. 2012.

[30] ITU-R. *P.676-11 Attenuation by atmospheric gases*. 2016.

[31] ITU-R. *P.838-3 Specific attenuation model for rain for use in prediction methods*. 2005.

[32] ITU-T. *G.8271 Time and phase synchronization aspects of telecommunication networks*. 2020.

[33] ITU-T. *G.8271.1 Precision time protocol telecom profile for phase/time synchronization with full timing support from the network*. 2020.

[34] Meilong Jiang et al. "Wireless Fronthaul for 5G and Future Radio Access Networks: Challenges and Enabling Technologies". In: *IEEE Wireless Communications* 29.2 (2022), pp. 108–114. DOI: 10.1109/MWC.003.2100482.

[35] Ping-Heng Kuo and Alain Mourad. "Millimeter wave for 5G mobile fronthaul and backhaul". In: *2017 European Conference on Networks*

and Communications (EuCNC). 2017, pp. 1–5. DOI: 10.1109/EuCNC.2017.7980750.

[36] Erik G. Larsson et al. "Massive MIMO for next generation wireless systems". In: *IEEE Communications Magazine* 52.2 (2014), pp. 186–195. DOI: 10.1109/MCOM.2014.6736761.

[37] Hien Quoc Ngo et al. *Ultra-Dense Cell-Free Massive MIMO for 6G: Technical Overview and Open Questions*. 2024. arXiv: 2401.03898.

[38] O-RAN Alliance. *Open Xhaul Transport Working Group 9 - Xhaul Transport Requirements v01.00*. 2021. URL: https://o-ran.org/specifications.

[39] Chathurika Ranaweera et al. "5G C-RAN With Optical Fronthaul: An Analysis From a Deployment Perspective". In: *Journal of Lightwave Technology* 36.11 (2018), pp. 2059–2068. DOI: 10.1109/JLT.2017.2782822.

[40] T. S. Rappaport et al. "Millimeter Wave Mobile Communications for 5G Cellular: It Will Work!" In: *IEEE Access* 1 (2013), pp. 335–349.

[41] Bashar Romanous et al. "Network densification: Challenges and opportunities in enabling 5G". In: *2015 IEEE 20th International Workshop on Computer Aided Modelling and Design of Communication Links and Networks (CAMAD)*. 2015, pp. 129–134. DOI: 10.1109/CAMAD.2015.7390494.

[42] G. Roveda and M. Costa. "Flexible Use of D Band Spectrum for 5G Transport: a Research Field Trial as Input to Standardization". In: *2018 IEEE 29th Annual International Symposium on Personal, Indoor and Mobile Radio Communications (PIMRC)*. 2018, pp. 800–804. DOI: 10.1109/PIMRC.2018.8580825.

[43] Muhammad Usman Sheikh et al. "X-Haul Solutions for Different Functional Split Options Using THz and Sub-THz Bands". In: *Proceedings of the 20th ACM International Symposium on Mobility Management and Wireless Access*. MobiWac '22. Montreal, Quebec, Canada: Association for Computing Machinery, 2022, pp. 47–53. ISBN: 9781450394802. DOI: 10.1145/3551660.3560921.

[44] Small Cell Forum. *5G nFAPI Specifications - SCF225.3.0*. 2022. URL: https://scf.io.

[45] Dave Townend et al. "A Unified Line-of-Sight Probability Model for Commercial 5G Mobile Network Deployments". In: *IEEE Transactions on Antennas and Propagation* 70.2 (2022), pp. 1291–1297. DOI: 10.1109/TAP.2021.3119099.

[46] Dave Townend et al. "Challenges and Opportunities in Wireless Fronthaul". In: *IEEE Access* 11 (2023), pp. 106607–106619. DOI: 10.1109/ACCESS.2023.3319073.

[47] Dave Townend et al. "Urban Wireless Multi-hop x-Haul for Future Mobile Network Architectures". In: *ICC 2022 - IEEE International Conference on Communications*. 2022, pp. 1883–1887. DOI: 10.1109/ICC45855.2022.9838366.

[48] Berktug Ustundag et al. "Low-Noise Amplifiers for W-Band and D-Band Passive Imaging Systems in SiGe BiCMOS Technology". In: *2018 Asia-Pacific Microwave Conference (APMC)*. 2018, pp. 651–653. DOI: 10.23919/APMC.2018.8617582.

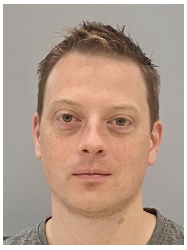

Dave Townend received the M.Eng degree in wireless communication engineering from Loughborough University, U.K., in 2007 and Ph.D in electronic systems engineering from the University of Essex, U.K., in 2024. He is currently a Wireless Research Manager at BT Laboratories and is a Chartered Engineer and a Member of the IET. His research interests include high frequency propagation, mobile network deployment modeling, transport network architecture and wireless backhaul.

Stuart D. Walker received the B.Sc. (Hons) degree in physics from Manchester University, U.K., in 1973, the M.Sc. degree in telecommunications systems and Ph.D. degree in electronics from Essex University, Colchester, U.K., in 1975 and 1981 respectively. From 1981-82, he was a post-doctoral research assistant at Essex University. From 1982-87, he was a research scientist at BT Laboratories, and from 1987-88 he was promoted to Group Leader in Submarine Systems Design. He joined Essex University in 1988 as a Senior Lecturer, and was promoted to Reader in 2002 and to Full Professor in 2004. At Essex University, he manages a laboratory concerned with all aspects of Access Networks: The Access Networks Group (ANG).

Anvar Tukmanov is a radio communication systems engineer. He received the B.Eng. degree in mobile communications from Kazan National Research Technical University, named after A.N.Tupolev, Russia, in 2007. He received his M.Sc. and Ph.D. in electrical engineering from Newcastle University, U.K., in 2009 and 2015, respectively. Anvar is currently the Head of Wireless Research at BT Labs, focusing on fundamental and emerging technologies increasing spectral and energy efficiency, and architectural flexibility of Radio Access Networks. Prior to that Anvar led research in MIMO communication systems applied to LTE and NR air interface technologies. He has been representing BT at 3GPP RAN1 working group since 2015. He is a recipient of the 2020 UKRI Future Leaders Fellowship and is a Distinguished Engineer at BT.

Andy Sutton is a Principal Network Architect in BT's Architecture and Technology Strategy team where he is responsible for radio access network (RAN) architecture evolution and mobile xhaul strategy. Andy holds an M.Sc. in mobile communications from the University of Salford and has 35 years of experience within the telecommunications industry. His research interests include distributed and centralised RAN architectures, optical and wireless transmission systems and mission critical network design and optimisation. Andy holds the post of Visiting Professor at the University of Liverpool and University of Salford, he's a Chartered Engineer and holds Fellowships from the IET, ITP and BCS. Andy sits on the editorial board of the Institute of Telecommunications Professionals Journal and has co-authored four books on telecommunications topics.